Neuro-Oncology
24(12), 2146–2158, 2022 | https://doi.org/10.1093/neuonc/noac136 | Advance Access date 24 May 2022

A comprehensive profiling of the immune microenvironment of breast cancer brain metastases

Gaia Griguolo[†], Anna Tosi[†], Maria Vittoria Dieci, Susan Fineberg, Valentina Rossi, Annavera Ventura, Michele Bottosso, Luc Bauchet, Federica Miglietta, Jack Jacob, Valerie Rigau, Matteo Fassan, William Jacot, PierFranco Conte, Antonio Rosato, Amelie Darlix, and Valentina Guarneri

Department of Surgery, Oncology and Gastroenterology, University of Padova, Padova, Italy (G.G., A.T., M.V.D., A.V., M.B., F.M., P.C., A.R., V.G.); Division of Oncology 2, Istituto Oncologico Veneto IRCCS, Padova, Italy (G.G., M.V.D., P.C., V.G.); Pathology Department, Albert Einstein College of Medicine/Montefiore Medical Center, Bronx, New York, USA (S.F.); Immunology and Molecular Oncology Diagnostics, Istituto Oncologico Veneto IRCCS, Padova, Italy (V.Ro., A.R.); Department of Neurosurgery, Gui de Chauliac Hospital—CHU, Montpellier University Medical Center, Montpellier, France (L.B.); Institute of Functional Genomics, Montpellier University, CNRS, INSERM, Montpellier, France (L.B.); Department of Pathology, Beth Israel Deaconess Medical Center and Harvard Medical School, Boston, Massachusetts, USA (J.J.); Department of Pathology, University of Montpellier, Montpellier, France (V.Ri.); Department of Medicine, Surgical Pathology Unit, University of Padova, Padova, Italy (M.F.); Istituto Oncologico Veneto IRCCS, Padova, Italy (M.F.); Medical Oncology Department, Institut du Cancer de Montpellier—University of Montpellier, Montpellier, France (W.J.); Medical Oncology Department, Institut du Cancer de Montpellier, Institut de Génomique Fonctionnelle, INSERM, CNRS—University of Montpellier, Montpellier, France (A.D.)

[†]Gaia Griguolo and Anna Tosi contributed equally as the first authors.

Corresponding Author: Valentina Guarneri, MD, PhD, Division of Oncology 2, Istituto Oncologico Veneto IRCCS, Via Gattamelata 64, 35128 Padova, Italy (valentina.guarneri@unipd.it).

Abstract

Background. Despite potential clinical implications, the complexity of breast cancer (BC) brain metastases (BM) immune microenvironment is poorly understood. Through multiplex immunofluorescence, we here describe the main features of BCBM immune microenvironment (density and spatial distribution) and evaluate its prognostic impact.

Methods. Sixty BCBM from patients undergoing neurosurgery at three institutions (2003-2018) were comprehensively assessed using two multiplex immunofluorescence panels (CD4, CD8, Granzyme B, FoxP3, CD68, pan-cytokeratin, DAPI; CD3, PD-1, PD-L1, LAG-3, TIM-3, CD163, pan-cytokeratin, DAPI). The prognostic impact of immune subpopulations and cell-to-cell spatial interactions was evaluated.

Results. Subtype-related differences in BCBM immune microenvironment and its prognostic impact were observed. While in HR–/HER2– BM and HER2+ BM, higher densities of intra-tumoral CD8+ lymphocytes were associated with significantly longer OS (HR 0.16 and 0.20, respectively), in HR+/HER2– BCBMs a higher CD4+FoxP3+/CD8+ cell ratio in the stroma was associated with worse OS (HR 5.4). Moreover, a higher density of intra-tumoral CD163+ M2-polarized microglia/macrophages in BCBMs was significantly associated with worse OS in HR–/HER2– and HR+/HER2– BCBMs (HR 6.56 and 4.68, respectively), but not in HER2+ BCBMs. In HER2+ BCBMs, multiplex immunofluorescence highlighted a negative prognostic role of PD-1/PD-L1 interaction: patients with a higher percentage of PD-L1+ cells spatially interacting with (within a 20 μm radius) PD-1+ cells presented a significantly worse OS (HR 4.60).

Conclusions. Our results highlight subtype-related differences in BCBM immune microenvironment and identify two potential therapeutic targets, M2 microglia/macrophage polarization in HER2– and PD-1/PD-L1 interaction in HER2+ BCBMs, which warrant future exploration in clinical trials.

Key Points

- Breast cancer brain metastases (BCBMs) immune microenvironment was evaluated by multiplex immunofluorescence.
- Subtype-related differences in immune subpopulations were observed.
- M2-polarized microglia/macrophages in HER2– and PD-1/PD-L1 interaction in HER2+ BCBMs represent potential targets.

Importance of the Study

Brain involvement is associated with poor prognosis and represents one of the major unmet needs in metastatic breast cancer (BC) care. Despite potential clinical implications, the complexity of brain metastases immune microenvironment in BC patients is still poorly understood. The comprehensive assessment of immune-related biomarkers through two multiplex immunofluorescence panels allowed us to highlight the significant interaction between immune microenvironment regulation and tumor biology in BC brain metastases, as we observed significant differences in the immune infiltrate composition and its prognostic role according to BC subtype. Our results highlighted subtype-related differences in immune regulation which should be taken into account when assessing potential therapeutic targets for immunotherapy in BC patients with brain metastases. We also identified two potential therapeutic targets, M2 microglia/macrophage polarization in HER2– and PD-1/PD-L1 interaction in HER2+ BC brain metastases, which warrant future exploration in translational studies and clinical trials.

Among solid tumors, breast cancer (BC) is one of the most common causes of brain metastases (BM). Brain involvement is associated with poor prognosis and represents a major unmet need in metastatic BC care. Indeed, approximately 10%-15% of metastatic BC patients will present clinically evident BM during the course of their disease.[1] Their frequency is higher in more aggressive BC subtypes: approximately 30% of human epidermal growth factor receptor type 2 (HER2)-positive and 50% of triple-negative (TNBC) metastatic patients will develop BMs.[2,3] Of note, these subtypes are also usually considered more immunogenic, with a higher mutational load and higher levels of tumor-infiltrating lymphocytes (TILs).[4]

Although the central nervous system (CNS) has been traditionally considered an immune-privileged sanctuary for cancers,[5] data from melanoma and lung cancer patients treated with immunotherapy have challenged this dogma and demonstrated a possible intracranial activity of immunotherapeutic agents.[6] Notwithstanding, the brain is an immune specialized site, endowed with additional hurdles to overcome before efficient immune response can be achieved.

As access to BM samples is complex, only a small number of studies have assessed the role of the immune system in BMs, the majority of them including patients with a variety of solid tumors.[7,8] In the largest study that evaluated the role of immune infiltrate specifically in BCBM patients, immune infiltrate was associated with improved survival, both overall and in the HER2+ subgroup.[9] A smaller study identified high levels of TILs to associate with better prognosis only in TNBC BMs patients.[10] Moreover, a third study not only reported PD-1+ TILs[11] to correlate with better prognosis in BCBM patients, particularly in the TNBC subgroup, but also identified CD68+ macrophage infiltration as an independent favorable prognostic factor,[11] thus highlighting the importance of a wider assessment of the immune microenvironment.

As various immunotherapeutic agents, including and beyond PD-1/PD-L1 inhibitors, are under clinical investigation in metastatic BC, a deeper knowledge of which are the molecular interactions and immune cells implicated in BC-related BMs (BCBMs) is required to inform the design of clinical trials in this setting. Moreover, a better understanding of whether these interactions are or are not subtype-specific is essential to define if such trials should be guided by BC subtype.

Multiplex immunofluorescence (mIF) is a novel approach that allows the simultaneous visualization and quantification of several proteins, plus nuclear counterstain, onto single FFPE (formalin-fixed paraffin-embedded) tissue sections, while maintaining tissue architecture and morphology. Through this technique, not only the density but also the functional state and the distribution of several types of immune cells within the tumor immune microenvironment (TIME) can be investigated.[12–16]

In this study, we applied mIF to comprehensively assess the immune microenvironment of BCBM samples and to characterize prognostically relevant immune subpopulations and cell-to-cell spatial interactions, with the ultimate goal of identifying biologically meaningful targets and inform future trials in this challenging clinical setting.

Materials and Methods

Patients

BC patients undergoing neurosurgery at three institutions between 2003 and 2018 were retrospectively identified.

This study was approved by involved Institutional Review Boards and Ethics Committees and conducted in accordance with the Declaration of Helsinki. Written informed consent was obtained from participants.

Clinical/anatomopathological data were collected from medical records. Hormone receptor (HR) and HER2 status were evaluated on primary tumor and on BCBM according to the guidelines (see Supplementary Methods).

Archival BCBM samples were centralized for analysis. Among these, this work has benefited from 450 white slides and the expertise of Professor Valérie Rigau responsible for the collections "Neurology" and "CEREMET-LR" of the Biological Resource Center of Montpellier University Hospital—http://www.chu-montpellier.fr (BB-0033-00031).[17]

Multiplex Immunofluorescence, Cell Density, and Cell-to-Cell Distance Analyses

After revision of each sample by a pathologist to confirm the presence of tumor cells and identify areas of necrosis, mIF staining was performed using the Opal seven-color manual kit (Akoya Biosciences). Two mIF panels were employed to characterize subsets of tumor-infiltrating immune cells. Before proceeding, optimal staining conditions for each marker were determined using monoplex stained slides from a positive control tissue (human tonsil) and then re-examined in a multiplex-stained BCBM tumor slide.

Multiplex slides were imaged using Mantra Quantitative Pathology Workstation (Akoya Biosciences) at ×20 magnification (only areas comprising tumor cells were considered). The inForm Image Analysis software (version 2.4.9, Akoya Biosciences) was used for analysis using representative multispectral images to train algorithms. Pan-cytokeratin (CK) staining was used to segment slides in tumor area and surrounding stroma; cell phenotyping was based on the detection of co-localized cell surface or intracellular markers. Cell density and percentage data were reported as the mean of all acquired fields from the same tissue slide (at least 20 fields at ×20 magnification for each slide), calculated in the tumor and stromal areas. Spatial metrics between cells (nearest neighbor analysis and count within analysis) were calculated using phenoptrReports (add-ins for R Studio from Akoya Biosciences) (Figure 1; see Supplementary Methods for more details).

Statistical Analysis

For statistical analysis, BC subtype evaluated on the BCBM was used. Differences in immune subpopulations across subgroups were tested using Mann-Whitney *U* tests or Kruskal-Wallis rank-sum tests, as adequate.

Survival analyses were conducted using the Kaplan-Meier method reported with 95% confidence intervals (95% CI). Median values were used to dichotomize immune variables in subgroups to investigate the association with survival using a log-rank test. Moreover, univariate Cox regression modeling was used to calculate HR and 95% CI. The prognostic role of each immune variable was evaluated both in the overall study cohort and in each BC subtype separately (TNBC, HR+/HER2–, HER2+). Due to the hypothesis-generating nature of this study, multiplicity correction was not used.

Analyses were performed using R software 3.6.1. and GraphPad Prism v7 (see Supplementary Methods).

Results

Patient and Tumor Characteristics

Sixty BC patients (all female) diagnosed with BM who underwent surgical resection between 2003 and 2018 at one of the participating institutions with evaluable samples for mIF analysis were included in this study: Centre Hospitalier Universitaire (CHU), Montpellier France (N = 22); Istituto Oncologico Veneto IRCCS, Padova Italy (N = 20); Montefiore Medical Center, Bronx NY, USA (N = 18) (REMARK flowchart, Supplementary Figure 2).

Patients' characteristics are reported in Table 1. Median age at time of primary tumor and BM diagnosis was 45 years (range 30-77) and 50 years (range 35-77), respectively. Median time from BC diagnosis to diagnosis of BM was 38.0 months (95% CI 29.0-61.6). BC subtyping on the BM was TNBC for 18 patients (30%), HR+/HER2– for 19 patients (31.7%), and HER2+ for 23 patients (38.3%). For patients with available HR status (N = 55) and HER2 status (N = 53) evaluated on primary BC, discordancy with receptor status evaluated on BM was observed in 20% (N = 11) of patients for HR (7 with loss of previous HR positivity and 4 with acquisition of HR positivity) and in 4% (N = 2) of patients for HER2 (both with acquisition of HER2 positivity).

Overall Survival From Brain Metastases Diagnosis and Clinical Characteristics

At a median follow-up of 42.6 months from BM diagnosis, 35 patients (58.3%) had died. Median overall survival (OS) from BM diagnosis (OS) was 33.4 months (95% CI 22.2-NR).

The only clinical variable associated with OS following BM diagnosis in this study cohort was BC subtype (median OS: 9.4 months for TNBC; 33.4 months for HR+/HER2–; 53.0 months for HER2+ BC; log-rank $P = .02$; Supplementary Figure 3), while the number of BM, performance status, and the presence/absence of extra-CNS disease at time of BM diagnosis were not significantly associated with survival outcome (univariate OS Cox models for these and other variables reported in Supplementary Table 1). Therefore, subsequent analyses testing the association of immune profiling and OS were also performed separately in each BC subtype.

Immune Profiling and Correlation With Brain Metastasis Breast Cancer Subtype

Each BCBM sample was analyzed using two mIF panels (Figure 1). The first was conceived to identify T lymphocytes (CD4+ and CD8+ cells), activated cytotoxic T lymphocytes (CD8+Granzyme B+ cells), T-regulatory cells (CD4+FoxP3+ cells), and microglia/macrophages (CD68+ cells) (Figure 1a).

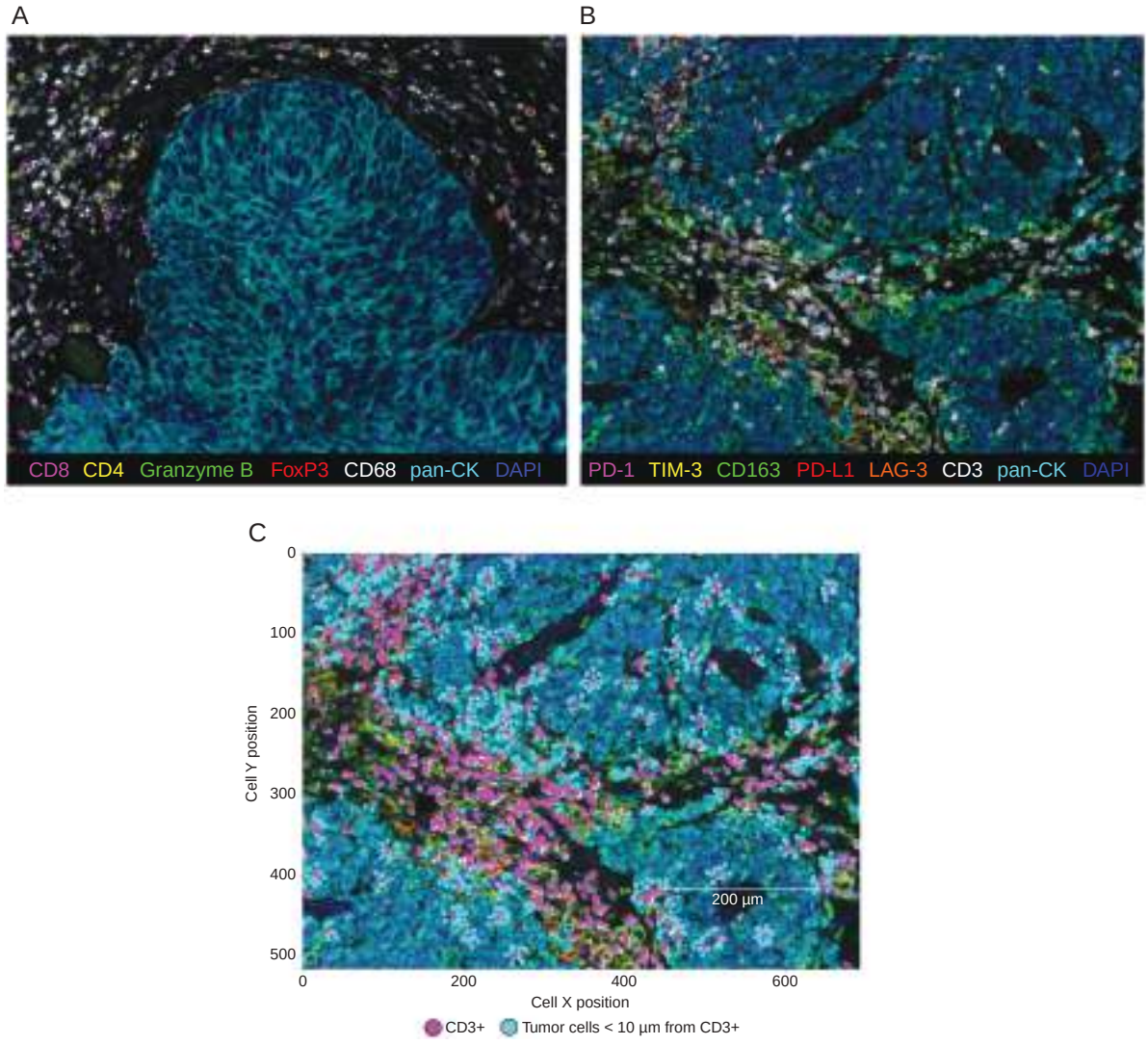

Fig. 1 mIF staining of BCBM. (a, b) Representative seven-color multispectral images of a BCBM sample stained with the first (a) and the second (b) mIF panels. Original magnification ×20. Immune markers and color codes are indicated in the legend. (c) Representative image of cell-cell distance analysis. Tumor cells (light blue dots) within a 10 µm radius from CD3+ cells (magenta dots) are represented. Abbreviations: BCBM, breast cancer brain metastases; mIF, multiplex immunofluorescence.

The second panel assessed the presence of immune checkpoint molecules, such as PD-1, LAG-3, and TIM-3 on immune cells and PD-L1 on both tumor and immune cells. CD163 marker was used to identify M2-polarized tumor-associated microglia/macrophages (Figure 1b). In both panels, pan-CK was used to identify the tumor and the stromal areas. Besides the quantification of each immune cell subtype, spatial analysis was also performed considering the XY coordinates of each cell (Figure 1c). Cells (tumor or immune cells) present within a maximum 30 µm radius from a cell with different phenotypes were considered interacting, as this radius represents an enhanced probability for cell-cell contact.[15]

Overall, immune infiltrate was mainly observed in the stroma as compared to the tumor area and was predominantly composed of CD68+ microglia/macrophages (Supplementary Figure 4a–c).

PD-1 and LAG-3 expression was detected only on CD3+ T cells in all BC subtypes (data not shown). In HER2– BCBM subtypes, PD-L1 was expressed mainly on CK+ tumor cells (around 60%) and on CD163+ microglia/macrophages (20%-25%), while in HER2+ BCBMs, PD-L1 was almost equally co-expressed by CK+ tumor cells, CD163+ microglia/macrophages and CD3+ T lymphocytes (Supplementary Figure 5a). Moreover, TIM-3 was mainly co-expressed by CD163+ microglia/macrophages (80%) in HER2+ and HR+/HER2– BCBMs, with CD3+ T cells being only the 10%-20% of TIM-3+ cells, while in TNBC BMs, TIM-3 was mainly detected on CD3+ T lymphocytes (55% among total TIM-3+ cells; Supplementary Figure 5b). Correlation between density of selected immune cell subpopulations are reported in Supplementary Tables 2–5.

Table 1. Patient Characteristics at Brain Metastases Diagnosis and Treatment Received

		n	%
Breast cancer subtype on brain metastases	TNBC	18	30.0
	HR+/HER2–	19	31.7
	HR+/HER2+	9	15.0
	HR–/HER2+	14	23.3
Number of BM	1	50	83.4
	2	5	8.3
	3 or more	5	8.3
Karnofsky performance status	100-90	15	31.9
	80-70	25	52.8
	60 or less	7	14.9
Brain metastases at time of first diagnosis of stage IV BC	Yes	39	67.2
	No	19	32.8
Presence of extra-CNS disease at time of brain metastases diagnosis	Yes	35	59.3
	No	24	40.7
Systemic therapy after brain metastases diagnosis	Yes	46	83.6
	No	9	16.4
Radiotherapy after brain metastases diagnosis	Yes	45	83.3
	No	9	16.7

Abbreviations: BC, breast cancer; BM, brain metastases; CNS, central nervous system; HER2, human epidermal growth factor receptor type 2; HR, hormone receptor; TNBC, triple-negative breast cancer.

Significant differences in immune cell populations between patients who received and patients who did not receive systemic treatment for metastatic BC before BM resection are reported in Supplementary Figure 6.

Significant differences in immune cell populations according to BC subtype were observed. HR+/HER2– BMs showed a higher density of CD68+ microglia/macrophages and a shorter distance between PD-L1+CK+ tumor cells and PD-1+CD3+T lymphocytes in the tumor area (Figure 2a and d), as compared to other BC subtypes. Similarly, in HR+/HER2– BMs, a shorter distance between PD-L1+CD163+ M2-polarized microglia/macrophages and PD-1+CD3+ T lymphocytes in the stroma was also observed (Figure 2e). On the other hand, TNBC BMs had a higher percentage of CD8+ cells co-expressing Granzyme B molecules within the tumor region (Figure 2b), as compared to the other BC subtypes. In the stroma area, a significant difference in TIM-3+ cell density was observed according to BC subtype, with the highest density in HR+/HER2– and lowest density in HER2+ tumors (Figure 2c).

Association Between BCBM Immune Cell Contexture and Survival in the Overall Study Cohort

The median value of each variable was calculated and was used as cutoff to stratify BCBMs into high and low subgroups. The intra-tumoral and stromal regions were analyzed independently.

In the overall study cohort, a low CD4+/CD8+ T-cell ratio (HR 0.55, 95% CI 0.28-1.09) and a low CD4+FoxP3+/CD8+ T-cell ratio (HR 0.55, 95% CI 0.28-1.08) in the stroma were associated with a longer OS (Figure 2f and g). Moreover, a lower percentage of CD4+FoxP3+ cells among total CD4+ cells within the tumor region was also indicative of a better prognosis (HR 0.41, 95% CI 0.20-0.85; Figure 2h). Considering the microglia/macrophage population, a higher density of intra-tumoral CD163+ M2-polarized microglia/macrophages was associated with a worse OS (HR 2.20, 95% CI 1.12-4.33; Figure 2i).

Distance analysis was performed to verify if particular cell-to-cell interactions had prognostic relevance in the overall study cohort, but no significant association was observed (data not shown).

Association Between Overall Survival and Immune Cell Contexture in TNBC BMs

Association between TIME contexture and patient prognosis was then evaluated separately in each BC subtype. Considering patients with TNBC BMs, high intra-tumoral densities of total CD3+ T cells (HR 0.23, 95% CI 0.06-0.94; Figure 3a), and in particular of CD8+ cytotoxic T lymphocytes (HR 0.16, 95% CI 0.03-0.85; Figure 3b), were associated to a prolonged OS as compared to patients with lower densities of these immune populations. Conversely, the negative prognostic impact of a higher density of intra-tumoral CD163+ M2-polarized microglia/macrophages was confirmed in the TNBC subtype (HR 6.56, 95% CI 1.35-31.77; Figure 3c). Paradoxically, a higher percentage of intra-tumoral CD163+PD-L1+ microglia/macrophages among total CD163+ microglia/macrophages was associated with

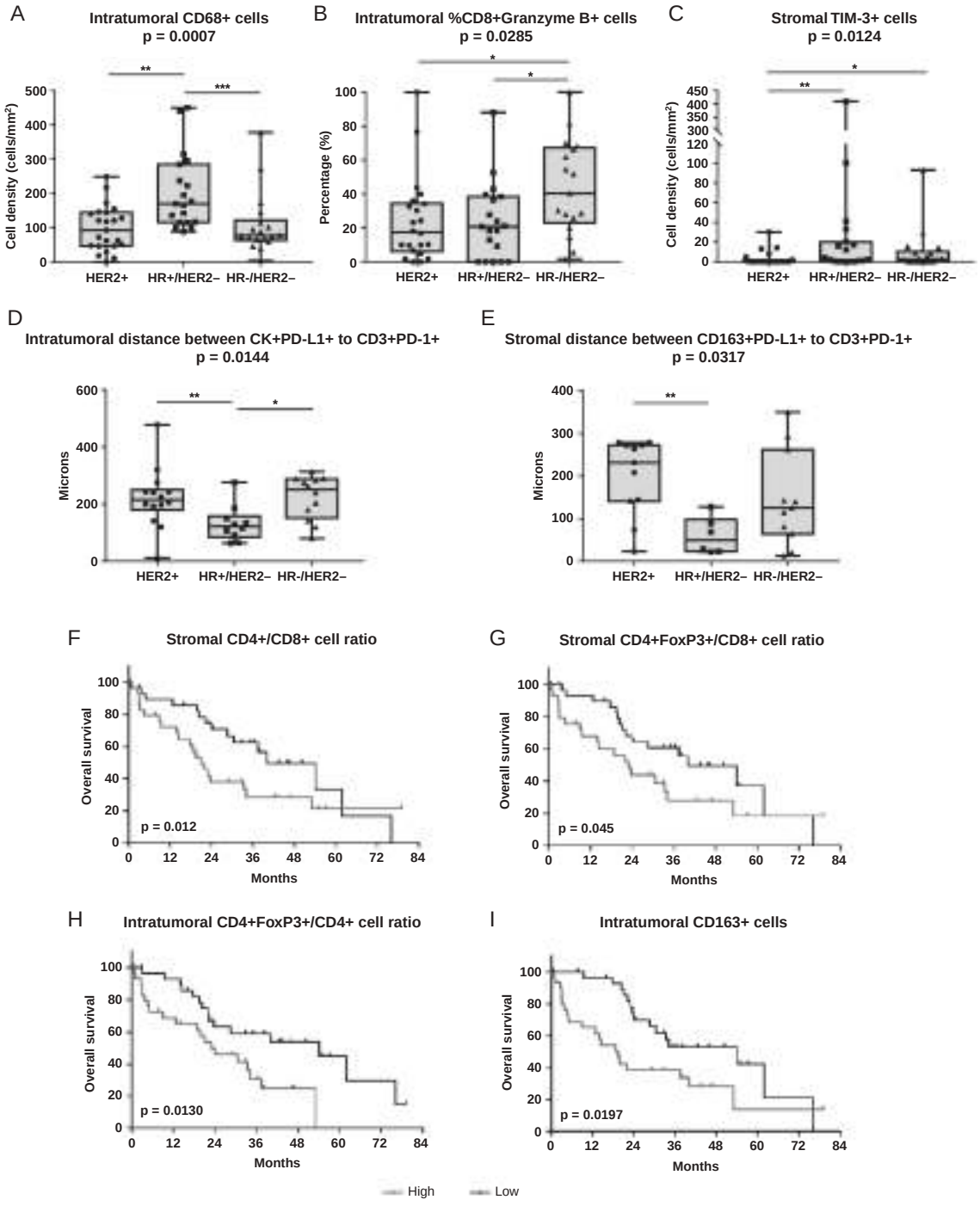

Fig. 2 Significant differences in immune infiltrate according to BCBM subtype and associations between BCBM immune cell composition and overall survival in the overall study cohort. (a–c) Significant differences in immune cell subpopulations infiltrating the stromal and the intratumoral regions according to BCBM subtype. Data are presented as (a, c) cell density (number of cells/mm^2) or (b) as cell percentage among total CD8+ cells. (d) Mean distance (μm) between each PD-L1+ tumor cell and the nearest PD-1+ T lymphocytes within the tumor region according to BCBM subtype. (e) Mean distance (μm) between each PD-L1+ M2-polarized macrophage and the nearest PD-1+ T lymphocytes in the stromal compartment according to BCBM subtype. Floating box shows median, 25th to 75th percentiles, and smallest to largest values. Nonparametric Mann-Whitney statistical analysis was performed, and significantly different data are represented by $^*P < .05$, $^{**}P < .01$, and $^{***}P < .001$. (f–i) Kaplan-Meier curves for OS according to (f) stromal CD4+/CD8+ T-cell ratio, (g) stromal CD4+FoxP3+/CD8+ T-cell ratio, (h) intra-tumoral CD4+FoxP3+/CD4+ T-cell ratio, and (i) intra-tumoral density of CD163+ M2-polarized macrophages in BCBM of overall study cohort. Median value of each variable was used as cutoff. Log-rank *P*-values are reported in each graph. Abbreviations: BCBM, breast cancer brain metastases; OS, overall survival; PD-1, programmed cell death-1; PD-L1, programmed cell death ligand 1.

a better OS (HR 0.19, 95% CI 0.05-0.73; Figure 3d). This was not linked to a specific association between density of intra-tumoral CD163+PD-L1+ microglia/macrophages and OS, but might potentially be explained by the positive correlation between density of intra-tumoral CD8+ cells and percentage of intra-tumoral CD163+ microglia/macrophages expressing PD-L1+ (r = 0.73, 95% CI 0.11-0.32, P = .0006; a similar association was also observed with the density of intra-tumoral CD163+PD-L1+ microglia/macrophages), while no significant association was observed between density of intra-tumoral CD8+ cells and global density of intra-tumoral CD163+ microglia/macrophages.

In addition, we also observed that several spatial interactions (as evaluated by distance analysis) had a significant prognostic value in TNBC BMs. In fact, a higher percentage of CD8+Granzyme B+ activated cytotoxic T cells within a 10 μm radius from tumor cells was associated with a prolonged OS (Figure 3g). Moreover, a higher percentage of FoxP3+ cells or CD68+ microglia/macrophages in close proximity to CD8+ T cells was also favorably associated with OS (Figure 3e, h, and i). For most of these associations, the prognostic impact was more evident when a shorter radius was considered, highlighting the biologic relevance of cell-cell proximity (Figure 3). These observations highlight that the generalized activation of the immune system observed in TNBC BMs often involves inhibitory immune components, potentially as a reaction to activation/upregulation of cytotoxic immune components.

Consistently, patients with a higher percentage of CD163+ microglia/macrophages within a 10 μm radius from CD3+ cells had a prolonged OS (Figure 3j) and a shorter distance between CD163+PD-L1+ microglia/macrophages and CD3+PD-1+T lymphocytes was associated with a better OS (HR 0.09 95% CI 0.01-0.49; Figure 3f), a further confirmation of the strong association between inhibitory and cytotoxic immune components in TNBC BMs.

Prognostic impact of other immune subpopulations (non-significant) is reported in Supplementary Figure 7.

Association Between Overall Survival and Immune Cell Contexture in HER2+ BCBMs

In HER2+ BCBMs, inhibitory checkpoint molecules appeared to play a crucial role in defining patient prognosis. In fact, higher densities of TIM-3+CD163+ microglia/macrophages both in the stroma (HR 3.55, 95% CI 1.08-11.68; Figure 4a) and intra-tumoral regions (HR 3.76, 95% CI 1.06-13.25; Figure 4b) were associated with worse OS in this subgroup. Moreover, the spatial interaction between PD-1 and PD-L1 was particularly relevant: patients with a higher percentage of PD-L1+ cells near (within a 20 μm radius) PD-1+ cells in the total sample area experienced a significantly worse prognosis (Figure 4e). This effect was mainly driven by the interaction between PD-L1+CD163+ microglia/macrophages and PD-1+CD3+ lymphocytes (Figure 4f and g). A similar negative prognostic effect of PD-1/PD-L1 interaction was observed in both tumor and stromal areas (Supplementary Figures 8 and 9).

A positive prognostic impact of CD8+ infiltrate was observed in this subtype as well: HER2+ patients with a higher density of intra-tumoral CD8+ cells had a better OS (HR 0.20, 95% CI 0.04-0.94; Figure 4c). In particular, patients with a shorter distance between CD8+Granzyme B+ activated T lymphocytes and tumor cells (HR 0.16, 95% CI 0.04-0.65; Figure 4d) and a higher percentage of activated CD8+Granzyme B+ T lymphocytes within a 30 μm radius from tumor cells (Figure 4h) showed a prolonged outcome.

Prognostic impact of other immune subpopulations (non-significant) is reported in Supplementary Figure 10.

Association Between Overall Survival and Immune Cell Contexture in HR+/HER2− BCBMs

In HR+/HER2− BC subtype, the negative prognostic impact of a higher density of CD163+ M2-polarized microglia/macrophages in the intra-tumoral region (HR 4.68, 95% CI 1.31-16.68; Figure 5a) was confirmed. In the stromal area, a high stromal density of TIM-3+ cells (mainly represented by TIM-3+CD163+ M2-polarized microglia/macrophages) was associated with a prolonged OS (HR 0.16, 95% CI 0.03-0.79; Figure 5b), while a higher CD4+FoxP3+/CD8+ cell ratio in the stroma was associated with worse outcome (HR 5.4, 95% CI 1.36-21.36; Figure 5c).

Consistently with what was observed in TNBC BMs, a spatial proximity (10-30 μm radius) between CD163+ cells and CD3+ cells was associated with better prognosis (HR 0.16, 95% CI 0.03-0.79, P = .011 for all distances between 10 and 30 μm).

Prognostic impact of other immune subpopulations (non-significant) is reported in Supplementary Figure 11.

Discussion

Over the last decade, increasing evidence has highlighted the relevance of immune regulation in metastatic BC, leading to the approval of immune checkpoint inhibitors in metastatic TNBC and to several trials testing their use in other BC subtypes. This article reports a comprehensive assessment of immune-related biomarkers in BCBMs and their association with patient prognosis in one of the largest BCBM cohorts published to date. In addition, the use of the mIF technique allowed us to highlight the prognostic role of spatial interaction between immune biomarkers in the context of BCBMs which could not be assessed by the use of immunohistochemistry (IHC) or bulk gene expression techniques. Indeed, given the key role of topologically distinct distribution of immune cells within the tumor microenvironment,[18] the mere analysis of the abundance of immune cells or their activation states is insufficient for a comprehensive characterization of the immune microenvironment of BCBMs.

In this study, BC subtype was the only clinical variable associated with OS after BM diagnosis, while other classic prognostic factors, such as performance status, did not reach significance probably due to the fact that this was a highly selected cohort of patients (all patients underwent neurosurgery). Consistently with previous reports, which have pointed out the significant interaction between immune microenvironment regulation and tumor biology in BC,[4,19–24] we observed significant differences in the

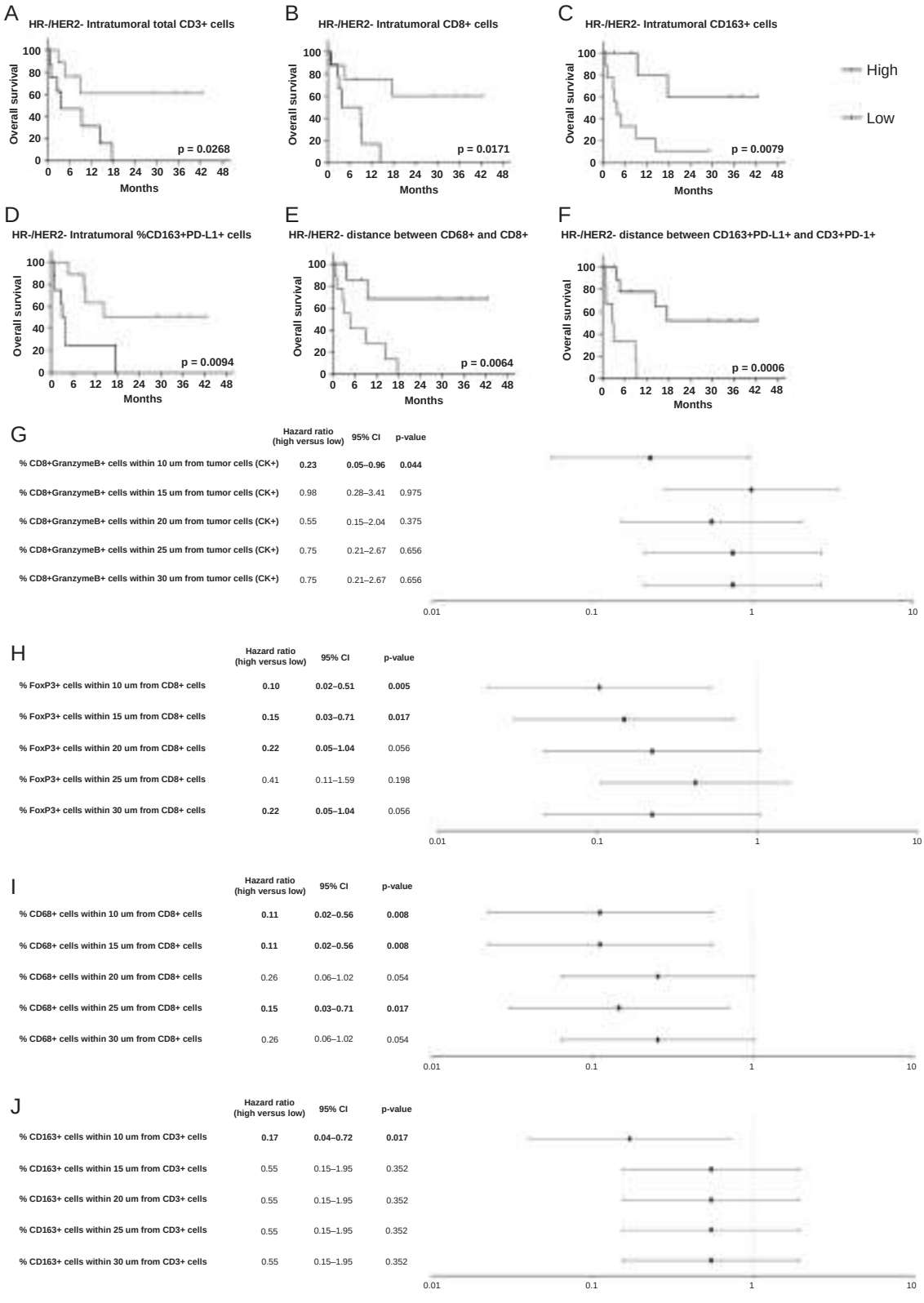

Fig. 3 Significant associations between immune contexture characteristics and overall survival and between cell-cell spatial interactions and overall survival in TNBC BMs cohort. Kaplan-Meier curves for OS according to (a) intra-tumoral density of total CD3+ T lymphocytes and (b) CD8+ T cells, (c) density of CD163+ M2-polarized macrophages in the intra-tumoral region, (d) percentage of CD163+ macrophages co-expressing

immune infiltrate composition and its prognostic role according to BC subtype.

Indeed, TNBC BMs showed a significantly higher percentage of intra-tumoral CD8+ cells co-expressing Granzyme B as compared to other subtypes, and a higher density of intra-tumoral CD8+ cells was associated with prolonged OS, in line with the general understanding that immune infiltrate in TNBC presents activated cytotoxic features and is associated with better outcome.[22,25] Using mIF we uncovered that, in TNBC BMs, several close interactions between cells (CD8+GranzymeB+ T cells with tumor cells; FoxP3+T_{reg} and CD68+ microglia/macrophages with CD8+T cells; CD163+ microglia/macrophages with CD3+ lymphocytes) were associated with better prognosis. These features underscore the prognostic relevance of a generalized activation of the immune system in this BC subtype and are consistent with the well-consolidated prognostic role of the immune infiltrate, as generically assessed by TILs, in TNBC,[21,22,26] and with a previous small study that identified low TIL levels in BCBM to be associated with worse OS in TNBC BMs patients specifically.[10]

In both HER2– BCBM subtypes of our cohort, a higher density of CD163+ M2-polarized microglia/macrophages within the tumor compartment was strongly associated with a worse prognosis. These data support the hypothesis that BC cells metastasizing to the brain might be able to hijack CNS microglia/macrophages and their cytoprotective mechanisms to facilitate metastatic growth.[27–31] Moreover, BCBMs have been reported to present higher levels of M2-polarized macrophages as compared to matched primary tumors.[32] Therefore, therapeutic manipulation of microglia/macrophages toward M1 polarization might potentially be exploited to achieve antitumor activity on BCBMs. Intriguingly, the PI3K pathway has been described to play a role in diverting microglia/macrophages toward a BM-promoting phenotype, and in BC models, the PI3K inhibitor buparlisib has been reported to drive macrophages toward the classical activated M1 phenotype.[27,31,33] Based on our observations, microglia/macrophage polarization warrants further exploration as a potential therapeutic target for BC patients with HER2– BMs, which currently represent one of the most relevant unmet needs in the treatment of metastatic BC.

Paradoxically, in both TNBC BMs and HR+/HER2– BCBMs, the interaction between CD163+ microglia/macrophages and T lymphocytes was associated with a better outcome. Moreover, in TNBC BMs a higher percentage of CD163+ microglia/macrophages co-expressing PD-L1 among total CD163+ microglia/macrophages present in the tumor region was associated with a prolonged OS, as well as the spatial proximity between PD-L1+ microglia/macrophages and PD-1+T lymphocytes. As we observed a strong correlation between intra-tumoral CD8+ cell density and the percentage of CD163+ cells expressing PD-L1 in this subtype, these results might in fact reflect an adaptive expression of the checkpoint molecule in response to the presence of a potentially active host antitumor immunological response.[22,34,35]

When considering the role of macrophages in BCBMs, it should be highlighted that the staining used in the present study (CD68, CD163) is unable to distinguish between resident activated microglia and peripheral macrophages recruited to the CNS. However, it has been reported that these two immune cell populations share similar morphology and functional states fluctuating across a pro- to anti-inflammatory function, depending on stimuli from local microenvironment, and might potentially be targeted by specific therapies (without distinction between these two cell populations).[27] Moreover, the M1/M2 dichotomization represents an oversimplification, and a spectrum of activation states exists with many cells displaying a mixed phenotype and M1- and M2-polarized macrophages representing the extremes of this spectrum. Although M2-polarized macrophages express several additional markers, such as CD206, CD204, and VEGF, the CD163 immunostaining is considered crucial to identify this pro-tumoral subpopulation[36] and most studies to date have used single or double immunostaining of macrophage markers, such as CD68 and CD163, to identify M1- or M2-polarized tumor-associated macrophages.[18,37]

In our study, the expression of the checkpoint molecule TIM-3 differently impacted patient prognosis based on BCBM subtype. Indeed, in HR+/HER2– BC patients, higher stromal density of TIM-3+ cells is associated with better prognosis, while in HER2+ BCBMs, a higher density of TIM-3-expressing microglia/macrophages is associated with worse outcome. These observations might appear contradictory, as TIM-3 is an immune checkpoint molecule with complex roles in the regulation of both innate and adaptive immune responses. It is generally described to be expressed on myeloid cells, natural killer cells, exhausted T cells, and regulatory T cells. It is often co-expressed with PD-1 and may play a role in resistance to PD-1 blockade.[38] Moreover, high TIM-3 expression has been described to be associated with worse survival in several solid tumors.[38–40] In BC, however, the prognostic significance of TIM-3 expression still remains unclear. A limited number of retrospective studies have reported a positive association between TIM-3 levels and survival in BC,[39–41] while in other works, TIM-3 expression was associated with poor response to neoadjuvant chemotherapy in locally advanced TNBC.[42] Moreover, the ligand-dependent functions

Fig. 3 Continued

PD-L1+ within the tumor region, (e, f) mean distance between (e) CD68+ macrophages and CD8+ T cells and (f) CD163+PD-L1+ M2-polarized macrophages and CD3+PD-1+ T lymphocytes. Median value of each variable was used as cutoff to identify high and low subgroups. Log-rank statistics were performed to determine significance; *P*-values are reported in each graph. (g–j) Univariate Cox model hazard ratios (HR), 95% confidence intervals (CI), and *P*-values for OS for percentage of tumor or immune cells present within 10, 15, 20, 25, and 30 µm radius from a cell with different phenotype in TNBC BMs. Median value of each variable was used as cutoff to identify high and low subgroups and HR for high vs low is reported. HR and 95% CI are represented. Bold characters indicate statistically significant cell interactions. Abbreviations: BMs, brain metastases; OS, overall survival; PD-1, programmed cell death-1; PD-L1, programmed cell death ligand 1; TNBC, triple-negative breast cancer.

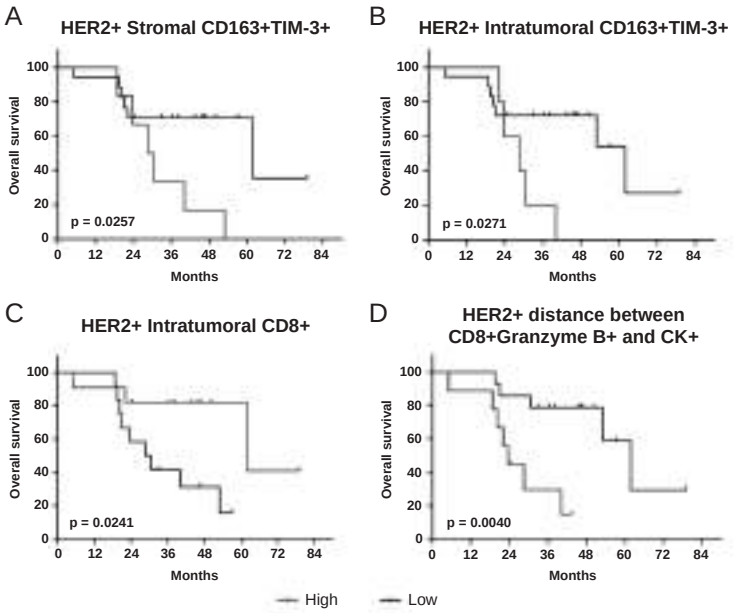

E

	Hazard ratio (high versus low)	95% CI	p-value
% PD-L1+ cells within 10 um from PD-1+ cells	2.35	0.71–7.78	0.163
% PD-L1+ cells within 15 um from PD-1+ cells	**4.60**	**1.19–17.68**	**0.027**
% PD-L1+ cells within 20 um from PD-1+ cells	**4.60**	**1.19–17.68**	**0.027**
% PD-L1+ cells within 25 um from PD-1+ cells	1.53	0.48–4.84	0.468
% PD-L1+ cells within 30 um from PD-1+ cells	2.31	0.69–7.66	0.174

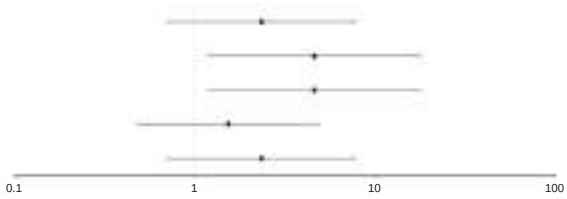

F

	Hazard ratio (high versus low)	95% CI	p-value
% PD-L1+ cells within 10 um from CD3+PD-1+ cells	2.87	0.87–9.44	0.084
% PD-L1+ cells within 15 um from CD3+PD-1+ cells	**5.51**	**1.44–21.04**	**0.012**
% PD-L1+ cells within 20 um from CD3+PD-1+ cells	**5.51**	**1.44–21.04**	**0.012**
% PD-L1+ cells within 25 um from CD3+PD-1+ cells	**5.51**	**1.44–21.04**	**0.012**
% PD-L1+ cells within 30 um from CD3+PD-1+ cells	2.83	0.85–9.45	0.091

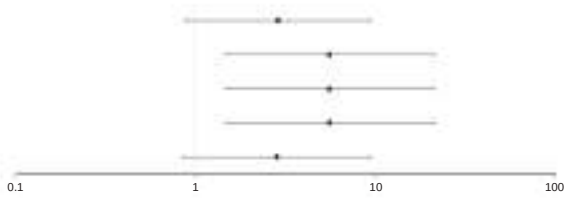

G

	Hazard ratio (high versus low)	95% CI	p-value
% CD163+PD-L1+ cells within 10 um from CD3+PD-1+ cells	2.63	0.69–10.09	0.159
% CD163+PD-L1+ cells within 15 um from CD3+PD-1+ cells	**4.99**	**1.45–17.10**	**0.011**
% CD163+PD-L1+ cells within 20 um from CD3+PD-1+ cells	**4.99**	**1.45–17.10**	**0.011**
% CD163+PD-L1+ cells within 25 um from CD3+PD-1+ cells	**4.02**	**1.17–13.85**	**0.027**
% CD163+PD-L1+ cells within 30 um from CD3+PD-1+ cells	1.77	0.57–5.56	0.326

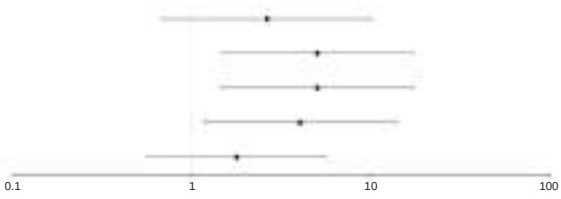

H

	Hazard ratio (high versus low)	95% CI	p-value
% CD8+GranzymeB+ cells within 10 um from tumor cells (CK+)	0.84	0.27–2.61	0.764
% CD8+GranzymeB+ cells within 15 um from tumor cells (CK+)	0.88	0.28–2.75	0.823
% CD8+GranzymeB+ cells within 20 um from tumor cells (CK+)	0.41	0.12–1.36	0.144
% CD8+GranzymeB+ cells within 25 um from tumor cells (CK+)	0.41	0.12–1.36	0.144
% CD8+GranzymeB+ cells within 30 um from tumor cells (CK+)	**0.22**	**0.06–0.84**	**0.027**

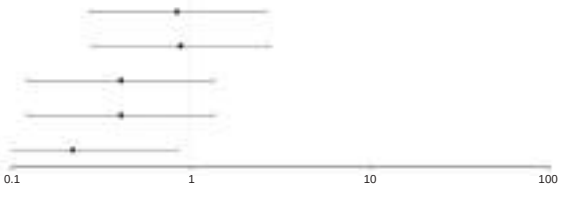

Fig. 4 Significant associations between immune contexture characteristics and overall survival and between cell-cell spatial interactions and overall survival in HER2+ BCBM cohort. Kaplan-Meier curves for OS according to (a) stromal and (b) intra-tumoral densities of TIM-3+ CD163+ M2-polarized macrophages, (c) intra-tumoral density of CD8+ T lymphocytes and (d) mean distance between CD8+ Granzyme B+ T lymphocytes

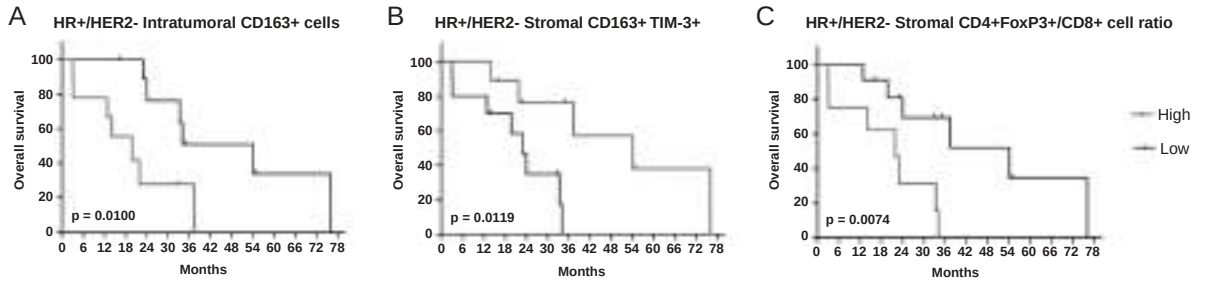

Fig. 5 Significant associations between immune cell infiltrate and overall survival in HR+/HER2– BCBM cohort. Kaplan-Meier curves for OS according to (a) intra-tumoral density of CD163+ M2-polarized macrophages, (b) stromal density of TIM-3+CD163+ macrophages, and (c) stromal CD4+FoxP3+/CD8+ cell ratio, in HR+/HER2– BCBM. Median value of each variable was used as cutoff. Log-rank *P*-values are reported in each graph. Abbreviations: BCBM, breast cancer brain metastases; HER2, human epidermal growth factor receptor type 2; HR, hormone receptor; OS, overall survival.

of TIM-3 are still unclear, as a pro-inflammatory effect that may favorably impact on patient outcome has been described.[43–45] In this context, the positive prognostic role of TIM-3+ cells in HR+/HER2– BCBMs observed in our cohort might be consistent with the general cognition of a more complex immune regulation and less straightforward prognostic impact of immune activation in this subtype, as compared to HR– and HER2+ BC.[19] In light of potential therapeutic implications, the role of TIM-3 in HR+/HER2– and in HER2+ BC subtypes warrants further exploration, as TIM-3-targeted immunotherapies are already being studied in clinical trials in combination with PD-1/PD-L1 inhibitors.[38]

Our study highlighted that in HER2+ BCBMs, the expression of immune checkpoints and their interactions appeared crucial for patient prognosis; this represented a peculiar feature of this BC subtype, potentially representing a possible target for combinatorial immunotherapies. Indeed, a higher number of PD-1+ T lymphocytes in close contact with PD-L1+ microglia/macrophages, both in tumor and stromal areas, was associated with worse OS in our cohort of HER2+ BCBM patients. We speculate that these observations might reflect the specific impact of HER2-targeted treatment on the immune microenvironment of HER2+ BC. It is well known that HER2-targeted antibodies achieve at least part of their antitumor activity by activating antibody-dependent cell-mediated cytotoxicity (ADCC).[23,46] Of note, while a rapid increase in tumor immune infiltration has been described as a consequence of HER2-targeted treatment in the early HER2+ BC setting,[16,47] the presence of high post-neoadjuvant TIL levels has been associated with impaired disease-free survival in early HER2+ BC with residual disease.[48] Indeed, the development of resistance to trastuzumab might, at least in part, be explained by the diversion of an initially inflamed immune microenvironment toward an exhausted phenotype through the upregulation of immune checkpoints, such as programmed cell death-1 (PD-1) and its ligand PD-L1.[49,50] As the large majority of HER2+ BC patients included in this study cohort had received previous HER2-targeted treatment, either in the neo/adjuvant or metastatic setting, interactions between PD-1 and PD-L1 molecules might represent an escape mechanism from antitumor immune activation generated by previous HER2-targeted treatment. Therefore, PD-1/PD-L1 inhibition in combination with HER2-targeted treatment might represent a promising potential therapeutic strategy for HER2+ BCBMs patients, and our data support the inclusion of patients with BMs in clinical trials testing this strategy in advanced HER2+ BC.

Collectively, in this study, we described the complexity of the immune microenvironment in BCBMs and assessed the prognostic role of immune cell populations and immune checkpoints in each BC subtype (TNBC, HR+/HER2–, HER2+). These are exploratory analyses conducted on a retrospective cohort of BCBM patients, and sample size for each BC subtype is limited, therefore warranting future validation in independent cohorts of BCBMs. Due to the hypothesis-generating nature of these analyses, multiplicity correction was not adopted, thus potentially increasing the risk of observing some false-positive results. Nevertheless, this study has several strengths: this BCBM cohort represents one of the largest studied to date, and was analyzed using mIF that allows not only the assessment of immune cells densities, but also of spatial metrics between immune biomarkers, thus allowing for the identification of biologically relevant interactions overlooked by other techniques.

Our results highlight that subtype-related differences in immune regulation should be taken into account in order

Fig. 4 Continued

and tumor cells. Median value of each variable was used as cutoff to identify high and low subgroups. Log-rank statistics were performed to determine significance; *P*-values are reported in each graph. (e–h) Univariate Cox model hazard ratios (HR), 95% confidence intervals (CI), and *P*-values for OS for percentage of immune populations present within 10, 15, 20, 25, and 30 µm radius from a cell with different phenotype or tumor cells in HER2+ BCBM. Median cutoff of each variable was used to separate high and low groups and HR for high vs low percentage is reported. Abbreviations: BCBM, breast cancer brain metastases; HER2, human epidermal growth factor receptor type 2; OS, overall survival.

to identify potential therapeutic targets for immunotherapy in BC patients with BM. Moreover, we identified two potential therapeutic targets, M2 microglia/macrophage polarization in HER2– BCBMs and PD-1/PD-L1 interaction in HER2+ BCBMs, which warrant future exploration in translational studies and clinical trials.

Supplementary Material

Supplementary material is available at *Neuro-Oncology* online.

Keywords

brain metastases | breast cancer | immune biomarkers | immune microenvironment | multiplex immunofluorescence

Funding

This study was funded by a 2019 Conquer Cancer Foundation of ASCO/Shanken Family Foundation Young Investigator Award to G.G. The authors also acknowledge grants from Fondazione AIRC under 5 per mille 2019—ID.22759 program—G.L. to V.G., A.R. and M.F.; Veneto Region and Italian Health Ministry's research program NET-2016-02363853 to P.F.C. and M.F.; Fondazione AIRC-IG 2018-ID. 2135 to A.R.; Italian Health Ministry's RCR-2019-23669115 to A.R.; Italian Health Ministry's NET-2016-02361632 to A.R.; Ricerca Corrent funding from the Italian Ministry of Health; Veneto Institute of Oncology IOV-IRCCS to M.V.D., P.F.C., A.R., and V.G.; DOR funding from the University of Padova to G.G., M.V.D., and V.G.

Conflict of interest statement. G.G. reports personal fees from Eli Lilly and Novartis. M.V.D. reports personal fees from Eli Lilly, Exact Sciences, Novartis, Pfizer, and Seagen. S.F. reports personal fees from AXDEV. W.J. reports grants from AstraZeneca; personal fees from AstraZeneca, Eisai, F. Hoffmann LaRoche, Lilly, MSD, Novartis, and Pfizer. P.F.C. reports grants (Institution) from Merck KGaA, Roche, and BMS; grants and personal fees from Novartis, Eli Lilly, AstraZeneca, Tesaro, BMS, and Roche; personal fees and grants (Institution) from BMS, Roche, and Novartis; personal fees from Eli Lilly, AstraZeneca, and Tesaro. V.G. reports personal fees from Novartis, Roche, Eli Lilly, and MSD. All reported COIs are outside the submitted work. The remaining authors declare no competing interests.

Authorship statement. Study design: G.G., M.V.D., P.F.C., and V.G. Acquisition of clinical data: G.G., M.V.D., S.F., M.B., L.B., F.M., J.J., V.Ri., W.J., A.D., P.F.C., and V.G. Translational analysis: A.T., V.Ro., A.V., M.F., and A.R. Data analysis and interpretation: G.G. and A.T. Manuscript drafting: G.G. and A.T. Manuscript revision: M.V.D., A.R., and V.G. Final approval of manuscript: all authors. G.G. and A.T. are co-first authors.

References

1. Lin NU, Bellon JR, Winer EP. CNS metastases in breast cancer. *J Clin Oncol*. 2004;22(17):3608–3617.
2. Bendell JC, Domchek SM, Burstein HJ, et al. Central nervous system metastases in women who receive trastuzumab-based therapy for metastatic breast carcinoma. *Cancer*. 2003;97(12):2972–2977.
3. Darlix A, Louvel G, Fraisse J, et al. Impact of breast cancer molecular subtypes on the incidence, kinetics and prognosis of central nervous system metastases in a large multicentre real-life cohort. *Br J Cancer*. 2019;121(12):991–1000.
4. Luen S, Virassamy B, Savas P, Salgado R, Loi S. The genomic landscape of breast cancer and its interaction with host immunity. *Breast*. 2016;29:241–250.
5. Dutoit V, Migliorini D, Dietrich P-Y, Walker PR. Immunotherapy of malignant tumors in the brain: how different from other sites? *Front Oncol*. 2016;6.
6. Lazaro T, Brastianos PK. Immunotherapy and targeted therapy in brain metastases: emerging options in precision medicine. *CNS Oncol*. 2017;6(2):139–151.
7. Harter PN, Bernatz S, Scholz A, et al. Distribution and prognostic relevance of tumor-infiltrating lymphocytes (TILs) and PD-1/PD-L1 immune checkpoints in human brain metastases. *Oncotarget*. 2015;6(38):40836–40849.
8. Berghoff AS, Fuchs E, Ricken G, et al. Density of tumor-infiltrating lymphocytes correlates with extent of brain edema and overall survival time in patients with brain metastases. *Oncoimmunology*. 2016;5(1):e1057388.
9. Sambade MJ, Prince G, Deal AM, et al. Examination and prognostic implications of the unique microenvironment of breast cancer brain metastases. *Breast Cancer Res Treat*. 2019;176(2):321–328.
10. Ogiya R, Niikura N, Kumaki N, et al. Comparison of immune microenvironments between primary tumors and brain metastases in patients with breast cancer. *Oncotarget*. 2017;8(61):103671–103681.
11. Duchnowska R, Pęksa R, Radecka B, et al. Immune response in breast cancer brain metastases and their microenvironment: the role of the PD-1/PD-L axis. *Breast Cancer Res*. 2016;18(1):43.
12. Stack EC, Wang C, Roman KA, Hoyt CC. Multiplexed immunohistochemistry, imaging, and quantitation: a review, with an assessment of Tyramide signal amplification, multispectral imaging and multiplex analysis. *Methods*. 2014;70(1):46–58.
13. Fridman WH, Zitvogel L, Sautès-Fridman C, Kroemer G. The immune contexture in cancer prognosis and treatment. *Nat Rev Clin Oncol*. 2017;14(12):717–734.
14. Feng Z, Puri S, Moudgil T, et al. Multispectral imaging of formalin-fixed tissue predicts ability to generate tumor-infiltrating lymphocytes from melanoma. *J Immunother Cancer*. 2015;3(1):47.
15. Carstens JL, Correa de Sampaio P, Yang D, et al. Spatial computation of intratumoral T cells correlates with survival of patients with pancreatic cancer. *Nat Commun*. 2017;8:15095.
16. Griguolo G, Serna G, Pascual T, et al. Immune microenvironment characterisation and dynamics during anti-HER2-based neoadjuvant treatment in HER2-positive breast cancer. *NPJ Precis Oncol*. 2021;5(1).
17. BB-0033-00031/Lames blanches/CRB/CHU de Montpellier, réseau BioBanques.
18. Hammerl D, Martens JWM, Timmermans M, et al. Spatial immunophenotypes predict response to anti-PD1 treatment and capture distinct paths of T cell evasion in triple negative breast cancer. *Nat Commun*. 2021;12(1):5668.

19. Dieci MV, Griguolo G, Miglietta F, Guarneri V. The immune system and hormone-receptor positive breast cancer: is it really a dead end? *Cancer Treat Rev.* 2016;46:9–19.
20. Denkert C, von Minckwitz G, Darb-Esfahani S, et al. Tumour-infiltrating lymphocytes and prognosis in different subtypes of breast cancer: a pooled analysis of 3771 patients treated with neoadjuvant therapy. *Lancet Oncol.* 2018;19(1):40–50.
21. Dieci MV, Radosevic-Robin N, Fineberg S, et al. Update on tumor-infiltrating lymphocytes (TILs) in breast cancer, including recommendations to assess TILs in residual disease after neoadjuvant therapy and in carcinoma in situ: a report of the International Immuno-Oncology Biomarker Working Group on Breast Cancer. *Semin Cancer Biol.* 2018;52:16–25.
22. Dieci MV, Tsvetkova V, Orvieto E, et al. Immune characterization of breast cancer metastases: prognostic implications. *Breast Cancer Res.* 2018;20(1):62.
23. Griguolo G, Pascual T, Dieci MV, Guarneri V, Prat A. Interaction of host immunity with HER2-targeted treatment and tumor heterogeneity in HER2-positive breast cancer. *J Immunother Cancer.* 2019;7(1):90.
24. Griguolo G, Dieci MV, Paré L, et al. Immune microenvironment and intrinsic subtyping in hormone receptor-positive/HER2-negative breast cancer. *NPJ Breast Cancer.* 2021;7(1):12.
25. Dieci MV, Tsvetkova V, Griguolo G, et al. Integration of tumour infiltrating lymphocytes, programmed cell-death ligand-1, CD8 and FOXP3 in prognostic models for triple-negative breast cancer: analysis of 244 stage I–III patients treated with standard therapy. *Eur J Cancer.* 2020;136:7–15.
26. Loi S, Drubay D, Adams S, et al. Tumor-infiltrating lymphocytes and prognosis: a pooled individual patient analysis of early-stage triple-negative breast cancers. *J Clin Oncol.* 2019;37(7):559–569.
27. Andreou KE, Soto MS, Allen D, et al. Anti-inflammatory microglia/macrophages as a potential therapeutic target in brain metastasis. *Front Oncol.* 2017;7.
28. Vidyarthi A, Agnihotri T, Khan N, et al. Predominance of M2 macrophages in gliomas leads to the suppression of local and systemic immunity. *Cancer Immunol Immunother.* 2019;68(12):1995–2004.
29. You H, Baluszek S, Kaminska B. Immune microenvironment of brain metastases—are microglia and other brain macrophages little helpers? *Front Immunol.* 2019;10.
30. You H, Baluszek S, Kaminska B. Supportive roles of brain macrophages in CNS metastases and assessment of new approaches targeting their functions. *Theranostics.* 2020;10(7):2949–2964.
31. Srinivasan ES, Tan AC, Anders CK, et al. Salting the soil: targeting the microenvironment of brain metastases. *Mol Cancer Ther.* 2021;20(3):455–466.
32. Zhu L, Narloch JL, Onkar S, et al. Metastatic breast cancers have reduced immune cell recruitment but harbor increased macrophages relative to their matched primary tumors. *J Immunother Cancer.* 2019;7(1):1–11.
33. Blazquez R, Wlochowitz D, Wolff A, et al. PI3K: a master regulator of brain metastasis-promoting macrophages/microglia. *Glia.* 2018;66(11):2438–2455.
34. Berry S, Taube JM. Innate vs. adaptive: PD-L1-mediated immune resistance by melanoma. *Oncoimmunology.* 2015;4(10):e1029704.
35. Kim HR, Ha SJ, Hong MH, et al. PD-L1 expression on immune cells, but not on tumor cells, is a favorable prognostic factor for head and neck cancer patients. *Sci Rep.* 2016;6:36956.
36. Etzerodt A, Moestrup SK. CD163 and inflammation: biological, diagnostic, and therapeutic aspects. *Antioxid Redox Signal.* 2013;18(17):2352–2363.
37. Jayasingam SD, Citartan M, Thang TH, et al. Evaluating the polarization of tumor-associated macrophages into M1 and M2 phenotypes in human cancer tissue: technicalities and challenges in routine clinical practice. *Front Oncol.* 2020;9.
38. Acharya N, Acharya N, Sabatos-Peyton C, Anderson AC, Anderson AC. Tim-3 finds its place in the cancer immunotherapy landscape. *J Immunother Cancer.* 2020;8(1):e000911.
39. Tu L, Guan R, Yang H, et al. Assessment of the expression of the immune checkpoint molecules PD-1, CTLA4, TIM-3 and LAG-3 across different cancers in relation to treatment response, tumor-infiltrating immune cells and survival. *Int J Cancer.* 2020;147(2):423–439.
40. Zang K, Hui L, Wang M, et al. TIM-3 as a prognostic marker and a potential immunotherapy target in human malignant tumors: a meta-analysis and bioinformatics validation. *Front Oncol.* 2021;11.
41. Burugu S, Gao D, Leung S, Chia SK, Nielsen TO. TIM-3 expression in breast cancer. *Oncoimmunology.* 2018;7(11):e1502128.
42. Cabioglu N, Onder S, Oner G, et al. TIM3 expression on TILs is associated with poor response to neoadjuvant chemotherapy in patients with locally advanced triple-negative breast cancer. *BMC Cancer.* 2021;21(1):357.
43. Han G, Chen G, Shen B, Li Y. Tim-3: an activation marker and activation limiter of innate immune cells. *Front Immunol.* 2013;4:449.
44. Koh HS, Chang CY, Jeon SB, et al. The HIF-1/glial TIM-3 axis controls inflammation-associated brain damage under hypoxia. *Nat Commun.* 2015;6(1):1–15.
45. Rodriguez-Manzanet R, Dekruyff R, Kuchroo VK, Umetsu DT. The costimulatory role of TIM molecules. *Immunol Rev.* 2009;229(1):259–270.
46. Bianchini G, Gianni L. The immune system and response to HER2-targeted treatment in breast cancer. *Lancet Oncol.* 2014;15(2):e58–e68.
47. Nuciforo P, Pascual T, Cortés J, et al. A predictive model of pathologic response based on tumor cellularity and tumor-infiltrating lymphocytes (CelTIL) in HER2-positive breast cancer treated with chemo-free dual HER2 blockade. *Ann Oncol.* 2018;29(1):170–177.
48. Hamy AS, Bonsang-Kitzis H, De Croze D, et al. Interaction between molecular subtypes and stromal immune infiltration before and after treatment in breast cancer patients treated with neoadjuvant chemotherapy. *Clin Cancer Res.* 2019;25(22):6731–6741.
49. Loi S, Giobbie-Hurder A, Gombos A, et al. Pembrolizumab plus trastuzumab in trastuzumab-resistant, advanced, HER2-positive breast cancer (PANACEA): a single-arm, multicentre, phase 1b-2 trial. *Lancet Oncol.* 2019;20(3):371–382.
50. Mittal D, Vijayan D, Neijssen J, et al. Blockade of ErbB2 and PD-L1 using a bispecific antibody to improve targeted anti-ErbB2 therapy. *Oncoimmunology.* 2019;8(11):e1648171.